

Measurement of the Λ_b^0 lifetime in the decay $\Lambda_b^0 \rightarrow J/\psi \Lambda^0$ with the DØ Detector

V.M. Abazov,³³ B. Abbott,⁷⁰ M. Abolins,⁶¹ B.S. Acharya,²⁷ M. Adams,⁴⁸ T. Adams,⁴⁶ M. Agelou,¹⁷ J.-L. Agram,¹⁸ S.H. Ahn,²⁹ M. Ahsan,⁵⁵ G.D. Alexeev,³³ G. Alkhazov,³⁷ A. Alton,⁶⁰ G. Alverson,⁵⁹ G.A. Alves,² M. Anastasoae,³² S. Anderson,⁴² B. Andrieu,¹⁶ Y. Arnaud,¹³ A. Askew,⁷⁴ B. Åsman,³⁸ O. Atramentov,⁵³ C. Autermann,²⁰ C. Avila,⁷ F. Badaud,¹² A. Baden,⁵⁷ B. Baldin,⁴⁷ P.W. Balm,³¹ S. Banerjee,²⁷ E. Barberis,⁵⁹ P. Bargassa,⁷⁴ P. Baringer,⁵⁴ C. Barnes,⁴⁰ J. Barreto,² J.F. Bartlett,⁴⁷ U. Bassler,¹⁶ D. Bauer,⁵¹ A. Bean,⁵⁴ S. Beauceron,¹⁶ M. Begel,⁶⁶ A. Bellavance,⁶³ S.B. Beri,²⁶ G. Bernardi,¹⁶ R. Bernhard,^{47,*} I. Bertram,³⁹ M. Besançon,¹⁷ R. Beuselinck,⁴⁰ V.A. Bezzubov,³⁶ P.C. Bhat,⁴⁷ V. Bhatnagar,²⁶ M. Binder,²⁴ K.M. Black,⁵⁸ I. Blackler,⁴⁰ G. Blazey,⁴⁹ F. Blekman,³¹ S. Blessing,⁴⁶ D. Bloch,¹⁸ U. Blumenschein,²² A. Boehnlein,⁴⁷ O. Boeriu,⁵² T.A. Bolton,⁵⁵ F. Borchering,⁴⁷ G. Borissov,³⁹ K. Bos,³¹ T. Bose,⁶⁵ A. Brandt,⁷² R. Brock,⁶¹ G. Brooijmans,⁶⁵ A. Bross,⁴⁷ N.J. Buchanan,⁴⁶ D. Buchholz,⁵⁰ M. Buehler,⁴⁸ V. Buescher,²² S. Burdin,⁴⁷ T.H. Burnett,⁷⁶ E. Busato,¹⁶ J.M. Butler,⁵⁸ J. Bystricky,¹⁷ W. Carvalho,³ B.C.K. Casey,⁷¹ N.M. Cason,⁵² H. Castilla-Valdez,³⁰ S. Chakrabarti,²⁷ D. Chakraborty,⁴⁹ K.M. Chan,⁶⁶ A. Chandra,²⁷ D. Chapin,⁷¹ F. Charles,¹⁸ E. Cheu,⁴² L. Chevalier,¹⁷ D.K. Cho,⁶⁶ S. Choi,⁴⁵ T. Christiansen,²⁴ L. Christofek,⁵⁴ D. Claes,⁶³ B. Clément,¹⁸ C. Clément,³⁸ Y. Coadou,⁵ M. Cooke,⁷⁴ W.E. Cooper,⁴⁷ D. Coppage,⁵⁴ M. Corcoran,⁷⁴ J. Coss,¹⁹ A. Cothenet,¹⁴ M.-C. Cousinou,¹⁴ S. Crépe-Renaudin,¹³ M. Cristetiu,⁴⁵ M.A.C. Cummings,⁴⁹ D. Cutts,⁷¹ H. da Motta,² B. Davies,³⁹ G. Davies,⁴⁰ G.A. Davis,⁵⁰ K. De,⁷² P. de Jong,³¹ S.J. de Jong,³² E. De La Cruz-Burelo,³⁰ C. De Oliveira Martins,³ S. Dean,⁴¹ F. Déliot,¹⁷ P.A. Delsart,¹⁹ M. Demarteau,⁴⁷ R. Demina,⁶⁶ P. Demine,¹⁷ D. Denisov,⁴⁷ S.P. Denisov,³⁶ S. Desai,⁶⁷ H.T. Diehl,⁴⁷ M. Diesburg,⁴⁷ M. Doidge,³⁹ H. Dong,⁶⁷ S. Doulas,⁵⁹ L. Duflot,¹⁵ S.R. Dugad,²⁷ A. Duperrin,¹⁴ J. Dyer,⁶¹ A. Dyshkant,⁴⁹ M. Eads,⁴⁹ D. Edmunds,⁶¹ T. Edwards,⁴¹ J. Ellison,⁴⁵ J. Elmsheuser,²⁴ J.T. Eltzroth,⁷² V.D. Elvira,⁴⁷ S. Eno,⁵⁷ P. Ermolov,³⁵ O.V. Eroshin,³⁶ J. Estrada,⁴⁷ D. Evans,⁴⁰ H. Evans,⁶⁵ A. Evdokimov,³⁴ V.N. Evdokimov,³⁶ J. Fast,⁴⁷ S.N. Fatakia,⁵⁸ L. Felgioni,⁵⁸ T. Ferbel,⁶⁶ F. Fiedler,²⁴ F. Filthaut,³² W. Fisher,⁶⁴ H.E. Fisk,⁴⁷ M. Fortner,⁴⁹ H. Fox,²² W. Freeman,⁴⁷ S. Fu,⁴⁷ S. Fuess,⁴⁷ T. Gadfort,⁷⁶ C.F. Galea,³² E. Gallas,⁴⁷ E. Galyaev,⁵² C. Garcia,⁶⁶ A. Garcia-Bellido,⁷⁶ J. Gardner,⁵⁴ V. Gavrilov,³⁴ P. Gay,¹² D. Gelé,¹⁸ R. Gelhaus,⁴⁵ K. Genser,⁴⁷ C.E. Gerber,⁴⁸ Y. Gershtein,⁷¹ G. Ginther,⁶⁶ T. Golling,²¹ B. Gómez,⁷ K. Gounder,⁴⁷ A. Goussiou,⁵² P.D. Grannis,⁶⁷ S. Greder,¹⁸ H. Greenlee,⁴⁷ Z.D. Greenwood,⁵⁶ E.M. Gregores,⁴ Ph. Gris,¹² J.-F. Grivaz,¹⁵ L. Groer,⁶⁵ S. Grünendahl,⁴⁷ M.W. Grunewald,²⁸ S.N. Gurzhiev,³⁶ G. Gutierrez,⁴⁷ P. Gutierrez,⁷⁰ A. Haas,⁶⁵ N.J. Hadley,⁵⁷ S. Hagopian,⁴⁶ I. Hall,⁷⁰ R.E. Hall,⁴⁴ C. Han,⁶⁰ L. Han,⁴¹ K. Hanagaki,⁴⁷ K. Harder,⁵⁵ R. Harrington,⁵⁹ J.M. Hauptman,⁵³ R. Hauser,⁶¹ J. Hays,⁵⁰ T. Hebbeker,²⁰ D. Hedin,⁴⁹ J.M. Heinmiller,⁴⁸ A.P. Heinson,⁴⁵ U. Heintz,⁵⁸ C. Hensel,⁵⁴ G. Hesketh,⁵⁹ M.D. Hildreth,⁵² R. Hirosky,⁷⁵ J.D. Hobbs,⁶⁷ B. Hoeneisen,¹¹ M. Hohlfield,²³ S.J. Hong,²⁹ R. Hooper,⁷¹ P. Houben,³¹ Y. Hu,⁶⁷ J. Huang,⁵¹ I. Iashvili,⁴⁵ R. Illingworth,⁴⁷ A.S. Ito,⁴⁷ S. Jabeen,⁵⁴ M. Jaffré,¹⁵ S. Jain,⁷⁰ V. Jain,⁶⁸ K. Jakobs,²² A. Jenkins,⁴⁰ R. Jesik,⁴⁰ K. Johns,⁴² M. Johnson,⁴⁷ A. Jonckheere,⁴⁷ P. Jonsson,⁴⁰ H. Jöstlein,⁴⁷ A. Juste,⁴⁷ M.M. Kado,⁴³ D. Käfer,²⁰ W. Kahl,⁵⁵ S. Kahn,⁶⁸ E. Kajfasz,¹⁴ A.M. Kalinin,³³ J. Kalk,⁶¹ D. Karmanov,³⁵ J. Kasper,⁵⁸ D. Kau,⁴⁶ R. Kehoe,⁷³ S. Kermiche,¹⁴ S. Kesisoglou,⁷¹ A. Khanov,⁶⁶ A. Kharchilava,⁵² Y.M. Kharzheev,³³ K.H. Kim,²⁹ B. Klima,⁴⁷ M. Klute,²¹ J.M. Kohli,²⁶ M. Kopal,⁷⁰ V.M. Korablev,³⁶ J. Kotcher,⁶⁸ B. Kothari,⁶⁵ A. Koubarovsky,³⁵ A.V. Kozelov,³⁶ J. Kozminski,⁶¹ S. Krzywdzinski,⁴⁷ S. Kuleshov,³⁴ Y. Kulik,⁴⁷ S. Kunori,⁵⁷ A. Kupco,¹⁷ T. Kurča,¹⁹ S. Lager,³⁸ N. Lahrichi,¹⁷ G. Landsberg,⁷¹ J. Lazoflores,⁴⁶ A.-C. Le Bihan,¹⁸ P. Lebrun,¹⁹ S.W. Lee,²⁹ W.M. Lee,⁴⁶ A. Leflat,³⁵ F. Lehner,^{47,*} C. Leonidopoulos,⁶⁵ P. Lewis,⁴⁰ J. Li,⁷² Q.Z. Li,⁴⁷ J.G.R. Lima,⁴⁹ D. Lincoln,⁴⁷ S.L. Linn,⁴⁶ J. Linnemann,⁶¹ V.V. Lipaev,³⁶ R. Lipton,⁴⁷ L. Lobo,⁴⁰ A. Lobodenko,³⁷ M. Lokajicek,¹⁰ A. Lounis,¹⁸ H.J. Lubatti,⁷⁶ L. Lueking,⁴⁷ M. Lynker,⁵² A.L. Lyon,⁴⁷ A.K.A. Maciel,⁴⁹ R.J. Madaras,⁴³ P. Mättig,²⁵ A. Magerkurth,⁶⁰ A.-M. Magnan,¹³ N. Makovec,¹⁵ P.K. Mal,²⁷ S. Malik,⁵⁶ V.L. Malyshev,³³ H.S. Mao,⁶ Y. Maravin,⁴⁷ M. Martens,⁴⁷ S.E.K. Mattingly,⁷¹ A.A. Mayorov,³⁶ R. McCarthy,⁶⁷ R. McCroskey,⁴² D. Meder,²³ H.L. Melanson,⁴⁷ A. Melnitchouk,⁶² M. Merkin,³⁵ K.W. Merritt,⁴⁷ A. Meyer,²⁰ H. Miettinen,⁷⁴ D. Mihalcea,⁴⁹ J. Mitrevski,⁶⁵ N. Mokhov,⁴⁷ J. Molina,³ N.K. Mondal,²⁷ H.E. Montgomery,⁴⁷ R.W. Moore,⁵ G.S. Muanza,¹⁹ M. Mulders,⁴⁷ Y.D. Mutaf,⁶⁷ E. Nagy,¹⁴ M. Narain,⁵⁸ N.A. Naumann,³² H.A. Neal,⁶⁰ J.P. Negret,⁷ S. Nelson,⁴⁶ P. Neustroev,³⁷ C. Noeding,²² A. Nomerotski,⁴⁷ S.F. Novaes,⁴ T. Nunnemann,²⁴ E. Nurse,⁴¹ V. O'Dell,⁴⁷ D.C. O'Neil,⁵ V. Oguri,³ N. Oliveira,³ N. Oshima,⁴⁷ G.J. Otero y Garzón,⁴⁸ P. Padley,⁷⁴ N. Parashar,⁵⁶ J. Park,²⁹ S.K. Park,²⁹ J. Parsons,⁶⁵ R. Partridge,⁷¹ N. Parua,⁶⁷ A. Patwa,⁶⁸ P.M. Perea,⁴⁵ E. Perez,¹⁷ O. Peters,³¹

P. Pétroff,¹⁵ M. Petteni,⁴⁰ L. Phaf,³¹ R. Piegai,¹ P.L.M. Podesta-Lerma,³⁰ V.M. Podstavkov,⁴⁷ Y. Pogorelov,⁵² B.G. Pope,⁶¹ W.L. Prado da Silva,³ H.B. Prosper,⁴⁶ S. Protopopescu,⁶⁸ M.B. Przybycien,^{50,†} J. Qian,⁶⁰ A. Quadt,²¹ B. Quinn,⁶² K.J. Rani,²⁷ P.A. Rapidis,⁴⁷ P.N. Ratoff,³⁹ N.W. Reay,⁵⁵ S. Reucroft,⁵⁹ M. Rijssenbeek,⁶⁷ I. Ripp-Baudot,¹⁸ F. Rizatdinova,⁵⁵ C. Royon,¹⁷ P. Rubinov,⁴⁷ R. Ruchti,⁵² G. Sajot,¹³ A. Sánchez-Hernández,³⁰ M.P. Sanders,⁴¹ A. Santoro,³ G. Savage,⁴⁷ L. Sawyer,⁵⁶ T. Scanlon,⁴⁰ R.D. Schamberger,⁶⁷ H. Schellman,⁵⁰ P. Schieferdecker,²⁴ C. Schmitt,²⁵ A.A. Schukin,³⁶ A. Schwartzman,⁶⁴ R. Schwienhorst,⁶¹ S. Sengupta,⁴⁶ H. Severini,⁷⁰ E. Shabalina,⁴⁸ M. Shamim,⁵⁵ V. Shary,¹⁷ W.D. Shephard,⁵² D. Shpakov,⁵⁹ R.A. Sidwell,⁵⁵ V. Simak,⁹ V. Sirotenko,⁴⁷ P. Skubic,⁷⁰ P. Slattery,⁶⁶ R.P. Smith,⁴⁷ K. Smolek,⁹ G.R. Snow,⁶³ J. Snow,⁶⁹ S. Snyder,⁶⁸ S. Söldner-Rembold,⁴¹ X. Song,⁴⁹ Y. Song,⁷² L. Sonnenschein,⁵⁸ A. Sopczak,³⁹ M. Sosebee,⁷² K. Soustruznik,⁸ M. Souza,² B. Spurlock,⁷² N.R. Stanton,⁵⁵ J. Stark,¹³ J. Steele,⁵⁶ G. Steinbrück,⁶⁵ K. Stevenson,⁵¹ V. Stolin,³⁴ A. Stone,⁴⁸ D.A. Stoyanova,³⁶ J. Strandberg,³⁸ M.A. Strang,⁷² M. Strauss,⁷⁰ R. Ströhmer,²⁴ M. Strovink,⁴³ L. Stutte,⁴⁷ S. Sumowidagdo,⁴⁶ A. Sznajder,³ M. Talby,¹⁴ P. Tamburello,⁴² W. Taylor,⁵ P. Telford,⁴¹ J. Temple,⁴² S. Tentindo-Repond,⁴⁶ E. Thomas,¹⁴ B. Thooris,¹⁷ M. Tomoto,⁴⁷ T. Toole,⁵⁷ J. Torborg,⁵² S. Towers,⁶⁷ T. Trefzger,²³ S. Trincaz-Duvoid,¹⁶ B. Tuchming,¹⁷ C. Tully,⁶⁴ A.S. Turcot,⁶⁸ P.M. Tuts,⁶⁵ L. Uvarov,³⁷ S. Uvarov,³⁷ S. Uzunyan,⁴⁹ B. Vachon,⁵ R. Van Kooten,⁵¹ W.M. van Leeuwen,³¹ N. Varelas,⁴⁸ E.W. Varnes,⁴² I.A. Vasilyev,³⁶ M. Vaupel,²⁵ P. Verdier,¹⁵ L.S. Vertogradov,³³ M. Verzocchi,⁵⁷ F. Villeneuve-Seguié,⁴⁰ J.-R. Vlimant,¹⁶ E. Von Toerne,⁵⁵ M. Vreeswijk,³¹ T. Vu Anh,¹⁵ H.D. Wahl,⁴⁶ R. Walker,⁴⁰ L. Wang,⁵⁷ Z.-M. Wang,⁶⁷ J. Warchol,⁵² M. Warsinsky,²¹ G. Watts,⁷⁶ M. Wayne,⁵² M. Weber,⁴⁷ H. Weerts,⁶¹ M. Wegner,²⁰ N. Wermes,²¹ A. White,⁷² V. White,⁴⁷ D. Whiteson,⁴³ D. Wicke,⁴⁷ D.A. Wijngaarden,³² G.W. Wilson,⁵⁴ S.J. Wimpenny,⁴⁵ J. Wittlin,⁵⁸ M. Wobisch,⁴⁷ J. Womersley,⁴⁷ D.R. Wood,⁵⁹ T.R. Wyatt,⁴¹ Q. Xu,⁶⁰ N. Xuan,⁵² R. Yamada,⁴⁷ M. Yan,⁵⁷ T. Yasuda,⁴⁷ Y.A. Yatsunenko,³³ Y. Yen,²⁵ K. Yip,⁶⁸ S.W. Youn,⁵⁰ J. Yu,⁷² A. Yurkewicz,⁶¹ A. Zabi,¹⁵ A. Zatserklyaniy,⁴⁹ M. Zdrzil,⁶⁷ C. Zeitnitz,²³ D. Zhang,⁴⁷ X. Zhang,⁷⁰ T. Zhao,⁷⁶ Z. Zhao,⁶⁰ B. Zhou,⁶⁰ J. Zhu,⁵⁷ M. Zielinski,⁶⁶ D. Zieminska,⁵¹ A. Zieminski,⁵¹ R. Zitoun,⁶⁷ V. Zutshi,⁴⁹ E.G. Zverev,³⁵ and A. Zylberstejn¹⁷
(DØ Collaboration)

¹ *Universidad de Buenos Aires, Buenos Aires, Argentina*

² *LAFEX, Centro Brasileiro de Pesquisas Físicas, Rio de Janeiro, Brazil*

³ *Universidade do Estado do Rio de Janeiro, Rio de Janeiro, Brazil*

⁴ *Instituto de Física Teórica, Universidade Estadual Paulista, São Paulo, Brazil*

⁵ *Simon Fraser University, Burnaby, Canada, University of Alberta, Edmonton, Canada, McGill University, Montreal, Canada and York University, Toronto, Canada*

⁶ *Institute of High Energy Physics, Beijing, People's Republic of China*

⁷ *Universidad de los Andes, Bogotá, Colombia*

⁸ *Charles University, Center for Particle Physics, Prague, Czech Republic*

⁹ *Czech Technical University, Prague, Czech Republic*

¹⁰ *Institute of Physics, Academy of Sciences, Center for Particle Physics, Prague, Czech Republic*

¹¹ *Universidad San Francisco de Quito, Quito, Ecuador*

¹² *Laboratoire de Physique Corpusculaire, IN2P3-CNRS, Université Blaise Pascal, Clermont-Ferrand, France*

¹³ *Laboratoire de Physique Subatomique et de Cosmologie, IN2P3-CNRS, Université de Grenoble 1, Grenoble, France*

¹⁴ *CPPM, IN2P3-CNRS, Université de la Méditerranée, Marseille, France*

¹⁵ *Laboratoire de l'Accélérateur Linéaire, IN2P3-CNRS, Orsay, France*

¹⁶ *LPNHE, Universités Paris VI and VII, IN2P3-CNRS, Paris, France*

¹⁷ *DAPNIA/Service de Physique des Particules, CEA, Saclay, France*

¹⁸ *IReS, IN2P3-CNRS, Université Louis Pasteur, Strasbourg, France and Université de Haute Alsace, Mulhouse, France*

¹⁹ *Institut de Physique Nucléaire de Lyon, IN2P3-CNRS, Université Claude Bernard, Villeurbanne, France*

²⁰ *RWTH Aachen, III. Physikalisches Institut A, Aachen, Germany*

²¹ *Universität Bonn, Physikalisches Institut, Bonn, Germany*

²² *Universität Freiburg, Physikalisches Institut, Freiburg, Germany*

²³ *Universität Mainz, Institut für Physik, Mainz, Germany*

²⁴ *Ludwig-Maximilians-Universität München, München, Germany*

²⁵ *Fachbereich Physik, University of Wuppertal, Wuppertal, Germany*

²⁶ *Panjab University, Chandigarh, India*

²⁷ *Tata Institute of Fundamental Research, Mumbai, India*

²⁸ *University College Dublin, Dublin, Ireland*

²⁹ *Korea Detector Laboratory, Korea University, Seoul, Korea*

³⁰ *CINVESTAV, Mexico City, Mexico*

³¹ *FOM-Institute NIKHEF and University of Amsterdam/NIKHEF, Amsterdam, The Netherlands*

³² *University of Nijmegen/NIKHEF, Nijmegen, The Netherlands*

³³ *Joint Institute for Nuclear Research, Dubna, Russia*

- ³⁴*Institute for Theoretical and Experimental Physics, Moscow, Russia*
³⁵*Moscow State University, Moscow, Russia*
³⁶*Institute for High Energy Physics, Protvino, Russia*
³⁷*Petersburg Nuclear Physics Institute, St. Petersburg, Russia*
³⁸*Lund University, Lund, Sweden, Royal Institute of Technology and Stockholm University, Stockholm, Sweden and Uppsala University, Uppsala, Sweden*
³⁹*Lancaster University, Lancaster, United Kingdom*
⁴⁰*Imperial College, London, United Kingdom*
⁴¹*University of Manchester, Manchester, United Kingdom*
⁴²*University of Arizona, Tucson, Arizona 85721, USA*
⁴³*Lawrence Berkeley National Laboratory and University of California, Berkeley, California 94720, USA*
⁴⁴*California State University, Fresno, California 93740, USA*
⁴⁵*University of California, Riverside, California 92521, USA*
⁴⁶*Florida State University, Tallahassee, Florida 32306, USA*
⁴⁷*Fermi National Accelerator Laboratory, Batavia, Illinois 60510, USA*
⁴⁸*University of Illinois at Chicago, Chicago, Illinois 60607, USA*
⁴⁹*Northern Illinois University, DeKalb, Illinois 60115, USA*
⁵⁰*Northwestern University, Evanston, Illinois 60208, USA*
⁵¹*Indiana University, Bloomington, Indiana 47405, USA*
⁵²*University of Notre Dame, Notre Dame, Indiana 46556, USA*
⁵³*Iowa State University, Ames, Iowa 50011, USA*
⁵⁴*University of Kansas, Lawrence, Kansas 66045, USA*
⁵⁵*Kansas State University, Manhattan, Kansas 66506, USA*
⁵⁶*Louisiana Tech University, Ruston, Louisiana 71272, USA*
⁵⁷*University of Maryland, College Park, Maryland 20742, USA*
⁵⁸*Boston University, Boston, Massachusetts 02215, USA*
⁵⁹*Northeastern University, Boston, Massachusetts 02115, USA*
⁶⁰*University of Michigan, Ann Arbor, Michigan 48109, USA*
⁶¹*Michigan State University, East Lansing, Michigan 48824, USA*
⁶²*University of Mississippi, University, Mississippi 38677, USA*
⁶³*University of Nebraska, Lincoln, Nebraska 68588, USA*
⁶⁴*Princeton University, Princeton, New Jersey 08544, USA*
⁶⁵*Columbia University, New York, New York 10027, USA*
⁶⁶*University of Rochester, Rochester, New York 14627, USA*
⁶⁷*State University of New York, Stony Brook, New York 11794, USA*
⁶⁸*Brookhaven National Laboratory, Upton, New York 11973, USA*
⁶⁹*Langston University, Langston, Oklahoma 73050, USA*
⁷⁰*University of Oklahoma, Norman, Oklahoma 73019, USA*
⁷¹*Brown University, Providence, Rhode Island 02912, USA*
⁷²*University of Texas, Arlington, Texas 76019, USA*
⁷³*Southern Methodist University, Dallas, Texas 75275, USA*
⁷⁴*Rice University, Houston, Texas 77005, USA*
⁷⁵*University of Virginia, Charlottesville, Virginia 22901, USA*
⁷⁶*University of Washington, Seattle, Washington 98195, USA*

(Dated: November 10, 2018)

We present measurements of the Λ_b^0 lifetime in the exclusive decay channel $\Lambda_b^0 \rightarrow J/\psi\Lambda^0$, with $J/\psi \rightarrow \mu^+\mu^-$ and $\Lambda^0 \rightarrow p\pi^-$, the B^0 lifetime in the decay $B^0 \rightarrow J/\psi K_S^0$ with $J/\psi \rightarrow \mu^+\mu^-$ and $K_S^0 \rightarrow \pi^+\pi^-$, and the ratio of these lifetimes. The analysis is based on approximately 250 pb⁻¹ of data recorded with the DØ detector in $p\bar{p}$ collisions at $\sqrt{s}=1.96$ TeV. The Λ_b^0 lifetime is determined to be $\tau(\Lambda_b^0) = 1.22_{-0.18}^{+0.22}(\text{stat}) \pm 0.04(\text{syst})$ ps, the B^0 lifetime $\tau(B^0) = 1.40_{-0.10}^{+0.11}(\text{stat}) \pm 0.03(\text{syst})$ ps, and the ratio $\tau(\Lambda_b^0)/\tau(B^0) = 0.87_{-0.14}^{+0.17}(\text{stat}) \pm 0.03(\text{syst})$. In contrast with previous measurements using semileptonic decays, this is the first determination of the Λ_b^0 lifetime based on a fully reconstructed decay channel.

PACS numbers: 14.20.Mr, 14.40.Nd, 13.30.Eg, 13.25.Hw

Calculations based on a simple quark-spectator model [1] predict that the lifetimes of all b hadrons are equal. When non-spectator effects are taken into account, they give rise to a lifetime hierarchy of $\tau(B^+) \geq$

$\tau(B^0) \approx \tau(B_s^0) > \tau(\Lambda_b^0) \gg \tau(B_c^+)$ [2]. Measurements of b -hadron lifetimes therefore provide means to determine the importance of non-spectator contributions in b -hadron decays. For comparison with theory, measure-

ments of lifetime ratios are preferred over individual lifetimes. The ratio $\tau(\Lambda_b^0)/\tau(B^0)$ has been the source of theoretical study since early calculations [3] predicted a value greater than 0.90, almost two sigma away from the measurement average [4], 0.800 ± 0.053 . Recent calculations [5] of this ratio that include higher order effects have reduced this difference. A current compilation [4] of lifetime ratio data for b hadrons is consistent with early calculations [6] that include non-spectator effects. Previous measurements of $\tau(\Lambda_b^0)$ used semileptonic decay channels that suffer from uncertainties arising from undetected neutrinos. A measurement of the lifetime using fully reconstructed Λ_b^0 decays is free from the neutrino ambiguities. The Tevatron Collider at Fermilab is the only operating accelerator where Λ_b^0 baryons are being produced and studied.

In this Letter we report a measurement of the Λ_b^0 lifetime in the decay channel $\Lambda_b^0 \rightarrow J/\psi\Lambda^0$, and its ratio to the B^0 lifetime from the $B^0 \rightarrow J/\psi K_S^0$ decay channel. This B^0 decay channel is chosen because of its similar topology to the Λ_b^0 decay. The J/ψ is reconstructed in the $\mu^+\mu^-$ decay mode, the Λ^0 in $p\pi^-$, and the K_S^0 in $\pi^+\pi^-$; throughout this Letter the appearance of a specific charge state will also imply its charge conjugate. The data used in this analysis were collected during 2002–2004 with the DØ detector in Run II of the Tevatron Collider at a center-of-mass energy of 1.96 TeV, and correspond to an integrated luminosity of approximately 250 pb^{-1} .

The components of the DØ detector [7] most relevant for this measurement are the charged-particle tracking systems and the muon detector. The DØ tracker consists of a silicon microstrip tracker (SMT) and a central fiber tracker (CFT) that are surrounded by a superconducting solenoid magnet that produces a 2 T central magnetic field. The SMT has approximately 800,000 individual strips, with a typical pitch of $50-80 \mu\text{m}$, and a design optimized for tracking and vertexing capability for $|\eta| < 3$ ($\eta = -\ln[\tan(\theta/2)]$ and θ is the polar angle). The system has a six-barrel longitudinal structure interspersed with sixteen disks. Each barrel consists of four layers arranged axially around the beam and the disks are placed perpendicular to the beam. The CFT has eight thin coaxial barrels, each supporting two doublets of overlapping scintillating fibers of 0.835 mm diameter, one doublet being parallel to the collision axis, and the other alternating by $\pm 3^\circ$ relative to the axis. For charged particles, the resolution for the distance of closest approach as provided by the tracking system is approximately $50 \mu\text{m}$ for tracks with $p_T \approx 1 \text{ GeV}/c$, and improves asymptotically to $15 \mu\text{m}$ for tracks with $p_T \geq 10 \text{ GeV}/c$, p_T is the component of the momentum perpendicular to the beam pipe. Preshower detectors and electromagnetic and hadronic calorimeters surround the tracker. A muon system is located beyond the calorimeter, and consists of multilayer drift chambers and scintillation trigger counters preceding 1.8 T toroidal magnets, followed by two similar layers

beyond the toroids. Muon identification for $|\eta| < 1$ relies on 10 cm wide drift tubes, while 1 cm mini-drift tubes are used for $1 < |\eta| < 2$.

Primary vertex (PV) candidates are determined for each event by minimizing a χ^2 function that depends on all the tracks in the event and a term that represents the beam spot constraint. The beam spot is the run-by-run average beam position, where a run typically lasts several hours. The beam spot is stable during the periods of time when the proton and antiproton beams are kept colliding continuously and can be used as a constraint for the primary vertex fit. The initial primary vertex candidate and its χ^2 are obtained using all tracks. Next, each track used in the χ^2 calculation is removed temporarily and the χ^2 is calculated again; if the χ^2 decreases by 9 or more, this track is discarded from the PV fit. This procedure is repeated until no more tracks can be discarded. Additional primary vertices are obtained by applying the same algorithm to the discarded tracks until no more vertices are found.

We base our data selection on defined objects such as charged tracks and muons. Although we do not require any specific trigger to select our sample, most of the events selected fire dimuon or single muon triggers. Preliminary selection of dimuon events requires the presence of at least two muons of opposite charge reconstructed in the tracker and the muon system. We require that at least one of the muon candidates consists of a central track, defined by hits in the SMT and CFT, matched with muon track segments in all three layers of the muon system. For the second muon, we require a central track matched with hits in at least the innermost layer of the muon system. The sample of $J/\psi \rightarrow \mu^+\mu^-$ candidates consists of events with at least two muons, with trajectories constrained in a fit to a common vertex. The fit must have a χ^2 probability greater than 1%, and the invariant mass of the dimuons must be in the range $2.80 < M_{\mu\mu} < 3.35 \text{ GeV}/c^2$. To reconstruct Λ_b^0 and B^0 candidates, the J/ψ events are examined for Λ^0 and K_S^0 candidates. The $\Lambda^0 \rightarrow p\pi^-$ candidates are required to have two tracks of opposite charge which must originate from a common vertex with a χ^2 probability greater than 1%. A candidate is selected if the mass of the proton-pion system after the vertex-constrained fit falls in the $1.100 < M_{p\pi} < 1.128 \text{ GeV}/c^2$ window. The proton mass is assigned to the track of higher momentum, and the p_T of the Λ^0 is required to be greater than $2.4 \text{ GeV}/c$. The $K_S^0 \rightarrow \pi^+\pi^-$ selection follows the same criteria, except that the mass window is $0.460 < M_{\pi\pi} < 0.525 \text{ GeV}/c^2$, and $p_T > 1.8 \text{ GeV}/c$.

We reconstruct the Λ_b^0 and B^0 by performing a constrained fit to a common vertex for either the Λ^0 or K_S^0 and the two muon tracks, with the latter constrained to the J/ψ mass of $3.097 \text{ GeV}/c^2$ [4]. Because of their long decay lengths, a significant fraction of Λ^0 and K_S^0 will decay outside the SMT. Therefore, to maintain good ef-

iciency, no SMT hits are required on the tracks of the decay particles. To reconstruct the Λ_b^0 (B^0), we first find the Λ^0 (K_S^0) decay vertex, and then extrapolate the momentum vector of the ensuing particle and form a vertex with it and the two muon tracks belonging to the J/ψ . The precision of the Λ_b^0 (B^0) vertex position is dominated by the two muon tracks from the J/ψ . If more than one candidate is found in the event, the candidate with the best χ^2 probability is selected as the Λ_b^0 (B^0) candidate.

We determine the lifetime of a Λ_b^0 or B^0 by measuring the distance traveled by each b -hadron candidate in a plane transverse to the beam direction, and then applying a correction for the Lorentz boost. We define the transverse decay length as $L_{xy} = \mathbf{L}_{xy} \cdot \mathbf{p}_T / p_T$ where \mathbf{L}_{xy} is the vector that points from the primary to the secondary vertex and \mathbf{p}_T is the transverse momentum vector of the b hadron. The proper decay length (PDL) for a b -hadron candidate is then given by:

$$\text{PDL} = \frac{L_{xy}}{(\beta\gamma)_T^B} = L_{xy} \frac{cM_B}{p_T}, \quad (1)$$

where $(\beta\gamma)_T^B$, and M_B are the transverse boost and the mass of the b hadron, respectively. In our measurement, the value of M_B in Eq. 1 is set to the PDG mass value of Λ_b^0 or B^0 [4]. In our final selection of Λ_b^0 and B^0 candidates, we require an error of less than 100 μm on the PDL and we also require a total momentum greater than 5 GeV/c .

We perform an unbinned likelihood fit to measure the Λ_b^0 and B^0 lifetimes. The inputs for the fit are the mass, PDL and PDL error of the candidates. Candidates with invariant masses in the range of 5.1 to 6.1 GeV/c^2 for the Λ_b^0 and 4.9 to 5.7 GeV/c^2 for the B^0 are selected; these ranges include sideband regions that are used to model the PDL distributions of backgrounds. The likelihood function, \mathcal{L} , is defined by:

$$\mathcal{L} = \prod_{j=1}^N [f_s S_M(M_j) S_L(\lambda_j, \sigma_j) + (1 - f_s) B_M(M_j) B_L(\lambda_j, \sigma_j)], \quad (2)$$

where N is the total number of selected events, f_s is the fraction of signal events in the sample, S_M and B_M are the probability distribution functions used to model the mass distributions for signal and background, respectively, and S_L and B_L model the distributions of proper decay lengths for signal and background. The mass for signal is modeled by a Gaussian distribution and the mass for background is described by a second-order polynomial. The PDL distribution for signal is described by the convolution of an exponential decay, whose decay constant is one of the parameters of the fit, with a resolution function represented by a single Gaussian function:

$$G(\lambda_j, \sigma_j) = \frac{1}{\sqrt{2\pi}s\sigma_j} \exp\left(\frac{-\lambda_j^2}{2(s\sigma_j)^2}\right), \quad (3)$$

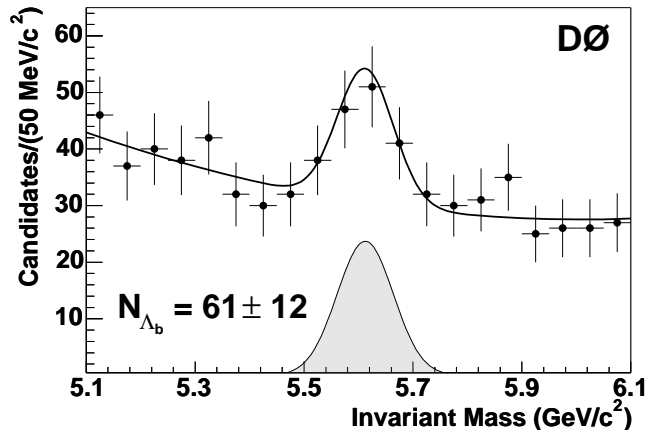


FIG. 1: Invariant mass distribution for Λ_b^0 candidate events. The points represent the data, and the curve represents the result of the fit. The mass distribution for the signal is shown in gray.

where λ_j and σ_j represent the PDL and its error respectively for a given event j , and the s parameter is introduced in the fit to account for a possible misestimate of σ_j . The PDL distribution for background is described by a sum of a resolution function representing the zero-lifetime component, negative and positive exponential decay functions modeling combinatorial background, and an exponential decay that accounts for long-lived heavy flavor decays. We minimize $-2 \ln \mathcal{L}$ to extract the parameters: $c\tau(\Lambda_b^0) = 366^{+65}_{-54} \mu\text{m}$ and $c\tau(B^0) = 419^{+32}_{-29} \mu\text{m}$. From the fits, we get $s = 1.27 \pm 0.10$ and $s = 1.39 \pm 0.05$ for the Λ_b^0 and B^0 respectively; and the number of signal events 61 ± 12 Λ_b^0 and 291 ± 23 B^0 . Figs 1 and 2 (Figs 3 and 4) show the mass and proper decay length distributions for the Λ_b^0 (B^0) candidates, respectively, with the results of the fits superimposed.

Table I summarizes the systematic uncertainties on our measurements. The contribution from the uncertainty on the detector alignment is estimated by reconstructing the B^0 sample with the positions of the SMT sensors shifted outwards radially by the alignment error in the radial position of the sensors and then fitting for the lifetime. We estimate the systematic uncertainty due to the resolution on the PDL by using two Gaussian functions for the resolution model. The contribution to the systematic uncertainty from the model describing background PDLs is studied by varying the parametrizations of the different components: (i) the exponential functions are replaced by exponentials convoluted with the resolution function of Eq. 3, (ii) a uniform background is added to account for outlier events (this has only a negligible effect), and (iii) the positive and negative short-lived lifetime components are forced to be symmetric. To study the systematic uncertainty due to the model for the mass distributions, we vary the shapes of the mass distribu-

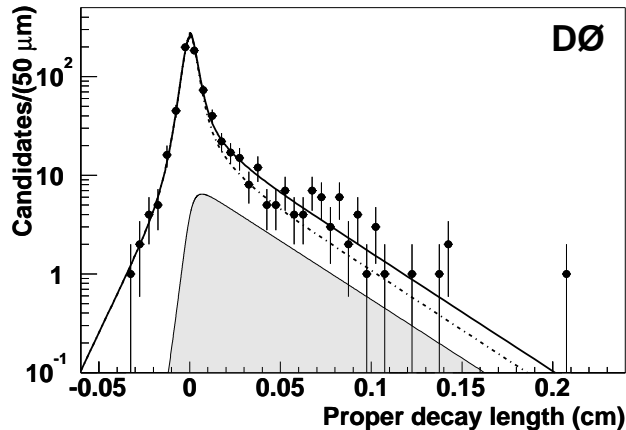


FIG. 2: Distribution of proper decay length for Λ_b^0 candidates. The points are the data, and the solid curve is the sum of the contributions from signal (gray) and the background (dashed-dotted line).

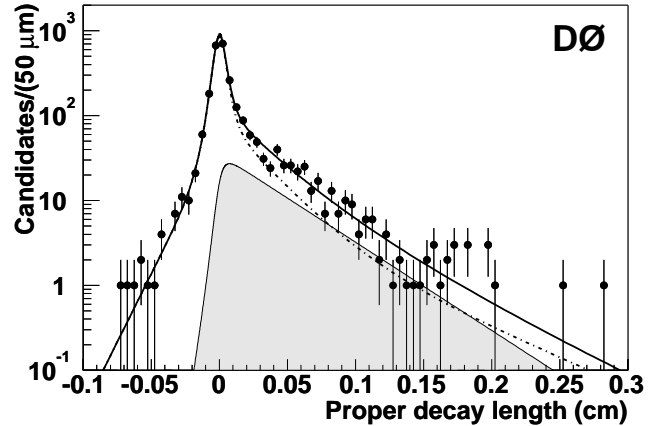


FIG. 4: Distribution of proper decay length for B^0 candidates. The points are the data, and the solid curve is the sum of the contributions from signal (gray) and the background (dashed-dotted line).

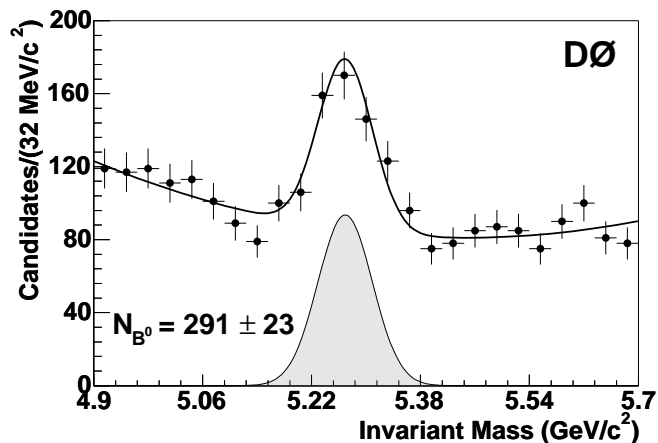


FIG. 3: Invariant mass distribution for B^0 candidate events. The points represent the data, and the curve represents the result of the fit. The mass distribution for the signal is shown in gray.

tions for signal and background. For the signal, we use two Gaussian functions instead of a single one, and for the background distribution, a linear function instead of the nominal quadratic form.

The lifetime of the long-lived component of the background varies with mass. This results in an uncertainty in the decay constant of the background under the mass peaks. We obtain the systematic uncertainty due to this effect by modelling the long-lived background with two exponentials instead of a single exponential. The decay constant of one of the two exponentials is determined from a fit in the low-mass sideband, and the other decay constant is determined from the high-mass sideband. The low-mass sideband is defined as the mass window $4.900\text{-}5.149\text{ GeV}/c^2$ for B^0 and $5.100\text{-}5.456\text{ GeV}/c^2$ for

Λ_b^0 and the high-mass sideband as $5.389\text{-}5.700\text{ GeV}/c^2$ and $5.768\text{-}6.100\text{ GeV}/c^2$ respectively. We perform the fit incorporating the linear combination of exponentials with the decay constants fixed to the values obtained in the low- and high-mass sidebands fits and allowing the coefficients of the linear combination to float. The systematic uncertainty quoted is the difference between the values we get from this fit and the nominal.

We also study the contamination of the Λ_b^0 sample by B^0 events that pass the Λ_b^0 selection. From Monte Carlo studies, we estimate that 19 B^0 events are reconstructed as Λ_b^0 events. The invariant masses of the B^0 events entering the Λ_b^0 sample are distributed almost uniformly across the entire mass range, and do not peak at the Λ_b^0 mass. Their proper decay lengths therefore tend to be incorporated in our model of the long-lived heavy-flavor component of the background. To estimate the systematic uncertainty due to this contamination, we fit the mass and proper decay length distributions of the misidentified events in the MC samples, add this contribution to the likelihood with fixed parameters, and perform the fit again. The difference between the two results is quoted as the systematic uncertainty due to the contamination.

The fitting procedure is tested for the presence of biases by generating 1000 Monte Carlo experiments, each with the same statistics as our data samples. For the generated events, the PDL errors are taken from data, and the mass and PDL distributions are described by the probability distribution functions used in data, with parameters obtained from the fit. The fits performed on these Monte Carlo experiments indicate that there is no bias inherent in the procedure.

We also perform several cross-checks of the lifetime measurements. In particular, a fit is done where the back-

TABLE I: Summary of systematic uncertainties in the measurement of $c\tau$ for Λ_b^0 and B^0 and their ratio. The total uncertainties are also given combining individual uncertainties in quadrature.

Source	Λ_b^0 (μm)	B^0 (μm)	Ratio
Alignment	5.4	5.4	0.002
Model for PDL resolution	6.7	2.7	0.010
Model for PDL background	2.7	3.1	0.005
Model for signal mass	0.2	0.0	0.000
Model for background mass	2.5	6.2	0.007
Long-lived components	1.5	0.1	0.003
Contamination	8.8	0.8	0.023
Total	12.9	9.2	0.028

ground is modeled using only sideband regions, the J/ψ vertex is used instead of the b -hadron vertex, the mass windows are varied, the reconstructed b -hadron mass is used instead of the Particle Data Group [4] value, and the sample is split into different pseudorapidity regions or different regions of azimuth. All results obtained with these variations are consistent with our central values.

The results of our measurement of the Λ_b^0 and B^0 lifetimes are summarized as:

$$\begin{aligned}\tau(\Lambda_b^0) &= 1.22_{-0.18}^{+0.22} \text{ (stat)} \pm 0.04 \text{ (syst)} \text{ ps}, \\ \tau(B^0) &= 1.40_{-0.10}^{+0.11} \text{ (stat)} \pm 0.03 \text{ (syst)} \text{ ps}.\end{aligned}\quad (4)$$

These can be combined to determine the ratio of lifetimes:

$$\frac{\tau(\Lambda_b^0)}{\tau(B^0)} = 0.87_{-0.14}^{+0.17} \text{ (stat)} \pm 0.03 \text{ (syst)}, \quad (5)$$

where we determine the systematic uncertainty of the ratio by varying each parameter in the two samples simultaneously and quoting the deviation in the ratio as the systematic uncertainty due to that source.

In conclusion, we have measured the Λ_b^0 lifetime in the fully reconstructed exclusive decay channel $J/\psi\Lambda_b^0$. This is the first time that this lifetime has been measured in an exclusive channel. The measurement is consistent with the world average, 1.229 ± 0.080 ps [4], and the Λ_b^0 to B^0 ratio of lifetimes is also consistent with theoretical predictions [3, 5, 6].

We thank the staffs at Fermilab and collaborating institutions, and acknowledge support from the Department of Energy and National Science Foundation (USA), Commissariat à l’Energie Atomique and CNRS/Institut National de Physique Nucléaire et de Physique des Particules (France), Ministry of Education and Science, Agency for Atomic Energy and RF President Grants Program (Russia), CAPES, CNPq, FAPERJ, FAPESP and FUNDUNESP (Brazil), Departments of Atomic Energy and Science and Technology (India), Colciencias (Colombia), CONACyT (Mexico), KRF (Korea), CONICET and UBACyT (Argentina), The Foundation for Fundamental Research on Matter (The Netherlands), PPARC (United Kingdom), Ministry of Education (Czech Republic), Natural Sciences and Engineering Research Council and WestGrid Project (Canada), BMBF and DFG (Germany), A.P. Sloan Foundation, Research Corporation, Texas Advanced Research Program, and the Alexander von Humboldt Foundation.

[*] Visitor from University of Zurich, Zurich, Switzerland.

[†] Visitor from Institute of Nuclear Physics, Krakow, Poland.

- [1] J. P. Leveille, in *Proceedings of the Ithaca B-decay Workshop, What Can We Hope To Learn From B Meson Decay*, (Univ. of Rochester, Ithaca, New York, 1981), UM HE 81-18.
- [2] I.I. Bigi, in *Proceedings of the 3rd International Conference on B Physics and CP Violation*, edited by H.-Y. Cheng and W.-S. Hou, (World Scientific, Singapore, 2000), hep-ph/0001003.
- [3] M. B. Voloshin, Phys. Rep. **320**, 275 (1999); B. Guberina, B. Melic, and H. Stefanic, Phys. Lett. B **469**, 253 (1999); M. Neubert and C.T. Sachrajda, Nucl. Phys. **B483**, 339 (1997).
- [4] S. Eidelman *et al.* (PDG), Phys. Lett. B **592**, 1 (2004).
- [5] C. Tarantino, Eur.Phys.J. **C 33**, s01, s895–s899 (2004), hep-ph/0310241.
- [6] N. Uraltsev, in *At the Frontier of Particle Physics: Handbook of QCD*, edited by M. Shifman (World Scientific, Singapore, 2001), hep-ph/0010328 (2001); G. Bellini, I.I. Bigi, P.J. Dornan, Phys. Rep. **289**, 1 (1997).
- [7] V. Abazov *et al.*, DØ Collaboration, “The Upgraded DØ Detector”, in preparation for submission to Nucl. Instrum. Methods Phys. Res. A; T. LeCompte and H.T. Diehl, “The CDF and DØ Upgrades for Run II,” Ann. Rev. Nucl. Part. Sci. **50**, 71 (2000).